© 2018. Published by The Company of Biologists Ltd | Journal of Cell Science (2018) 131, jcs222901. doi:10.1242/jcs.222901

RESEARCH ARTICLE

CCDC102B functions in centrosome linker assembly and centrosome cohesion

Yuqing Xia[1,*], Ning Huang[1,*], Zhiquan Chen[1], Fangyuan Li[1], Guiliang Fan[1], Dandan Ma[1], Jianguo Chen[1,2,‡] and Junlin Teng[1,‡]

ABSTRACT

The proteinaceous centrosome linker is an important structure that allows the centrosome to function as a single microtubule-organizing center (MTOC) in interphase cells. However, the assembly mechanism of the centrosome linker components remains largely unknown. In this study, we identify CCDC102B as a new centrosome linker protein that is required for maintaining centrosome cohesion. CCDC102B is recruited to the centrosome by C-Nap1 (also known as CEP250) and interacts with the centrosome linker components rootletin and LRRC45. CCDC102B decorates and facilitates the formation of rootletin filaments. Furthermore, CCDC102B is phosphorylated by Nek2A (an isoform encoded by *NEK2*) and is disassociated from the centrosome at the onset of mitosis. Together, our findings reveal a molecular role for CCDC102B in centrosome cohesion and centrosome linker assembly.

This article has an associated First Person interview with the first authors of the paper.

KEY WORDS: CCDC102B, Centrosome cohesion, C-Nap1, LRRC45, rootletin, Nek2A

INTRODUCTION

The centrosome is an essential organelle in animal cells that functions as the major microtubule-organizing center (MTOC); thus, it influences many microtubule-determined events, such as cell shape, cell polarity, spindle formation and cell division (Bornens, 2012; Lüders and Stearns, 2007; Nigg and Stearns, 2011). One centrosome consists of a mother centriole and a daughter centriole surrounded by the pericentriolar material (PCM) (Bornens, 2002) and is duplicated once per cell cycle before mitosis (Tsou and Stearns, 2006). Microtubules and actin filaments, which are regulated by their associated proteins, provide forces that hold the duplicated centrosomes together and prevent centrosome separation (Au et al., 2017; Decarreau et al., 2017; Panic et al., 2015). Furthermore, the duplicated centrosomes are connected from G1 to G2 phase as one MTOC by a physical linker, which is required for several cellular processes such as Golgi and cilia positioning (Mazo et al., 2016; Panic et al., 2015), and chromosome separation (Nam and van Deursen, 2014).

Several proteins, such as C-Nap1 (also known as CEP250), rootletin, LRRC45, Cep68 and β-catenin, have been previously reported to be centrosome linker components (Bahe et al., 2005; Bahmanyar et al., 2008; Graser et al., 2007; He et al., 2013; Mayor et al., 2000; Pagan et al., 2015; Yang et al., 2006). Among them, C-Nap1 is localized at the proximal ends of the centrioles and provides docking sites for filament-like proteins such as rootletin and LRRC45 (He et al., 2013; Panic et al., 2015; Yang et al., 2006). Both rootletin and LRRC45 can independently form filaments between the proximal ends of the centrioles through self-assembly, and this is required for centrosome cohesion (Bahe et al., 2005; He et al., 2013). Cep68 does not form filaments itself, rather, it links centrosomes in the shape of fiber-like structures in interphase and is connected to C-Nap1 through centlein, another centrosome linker component (Fang et al., 2014; Graser et al., 2007; Yang et al., 2006), and decorates the fibers formed by rootletin (Vlijm et al., 2018). Depletion of any of these centrosome linker proteins induces premature centrosome separation, also known as centrosome splitting (Mayor et al., 2000).

During the G2/M transition, the centrosome linker dissociates from the centrosome, and triggers centrosome separation and bipolar spindle formation (Mardin and Schiebel, 2012). The disassembly of the centrosome linker is mainly controlled by the balance between the protein kinase NIMA-related kinase 2A (Nek2A; an isoform encoded by *NEK2*) and phosphatase protein phosphatase 1 during mitosis (Helps et al., 2000; Meraldi and Nigg, 2001). Activated Nek2A phosphorylates centrosome linker proteins, such as rootletin, LRRC45 and Cep68, in the absence of phosphatase protein phosphatase 1 at the G2/M transition, which results in the disassociation of these linker proteins and finally causes centrosome separation (Bahe et al., 2005; Graser et al., 2007; He et al., 2013; Man et al., 2015; Mardin and Schiebel, 2012; Mayor et al., 2002; Nigg and Stearns, 2011).

Methylation in the promoter region of the gene encoding coiled-coil domain containing 102B (*CCDC102B*) is strongly associated with age, and may affect late-presenting right-sided diaphragmatic hernia and microphthalmia (Freire-Aradas et al., 2016; Park et al., 2016; Zayed et al., 2010). A recent study also found that CCDC102B is associated with myopic maculopathy (Hosoda et al., 2018). However, the detailed function of CCDC102B remains a mystery. In this study, we identify CCDC102B as a new centrosome linker protein, and reveal its roles in maintaining centrosome cohesion and centrosome linker assembly through cooperating with C-Nap1, Rootletin, Cep68 and LRRC45.

RESULTS

CCDC102B appears as fibers at the proximal ends of centrioles

Human CCDC102B is an uncharacterized protein containing 513 amino acids (aa); it is predicted to contain one short coiled-coil domain on its N-terminus and two long coiled-coil domains in the middle region and C-terminus, respectively (Fig. S1A). We first generated a polyclonal mouse antibody via immunization with a

[1]Key Laboratory of Cell Proliferation and Differentiation of the Ministry of Education and State Key Laboratory of Membrane Biology, College of Life Sciences, Peking University, Beijing 100871, China. [2]Center for Quantitative Biology, Peking University, Beijing 100871, China.
*These authors contributed equally to this work

‡Authors for correspondence (chenjg@pku.edu.cn; junlinteng@pku.edu.cn)

J.C., 0000-0002-8406-011X; J.T., 0000-0002-7611-0631

Received 19 July 2018; Accepted 30 October 2018

Journal of Cell Science (2018) 131, jcs222901. doi:10.1242/jcs.222901

GST-recombinant C-terminal fragment of human CCDC102B (217–513 aa). Immunoblots showed that the antibody recognized a band of ∼72 kDa, and this band was significantly reduced in the samples of cells transfected with small interfering RNAs (siRNAs) that targeted CCDC102B (Fig. S1B). The antibody also recognized exogenously expressed Flag–CCDC102B in U2OS cell lysates (Fig. S1C). Similar results were obtained with a commercial (GeneTex) antibody against CCDC102B (Fig. S1D).

To investigate the localization of CCDC102B in the cells, we co-immunostained CCDC102B and the centriole marker centrin-3 (hereafter centrin) in HeLa cells. CCDC102B was localized near to centrin in both G1 and G2 phases (Fig. 1A). Since centrin is localized at the distal lumen of the centrioles, CCDC102B is presumably enriched at the proximal ends. Thus, we co-immunostained CCDC102B and the centriole proximal-end marker C-Nap1. CCDC102B was partially colocalized with C-Nap1 in HeLa cells, confirming our hypothesis (Fig. 1B, upper panel). Interestingly, instead of the punctate structure we observed in HeLa cells, CCDC102B appeared more like 'fibers' between the centrosomes in U2OS cells (Fig. 1B, lower panel), similar to the characterization of rootletin (Bahe et al., 2005; Yang et al., 2006). We then co-immunostained CCDC102B and rootletin, and found that they were well colocalized with each other (Fig. 1C). Furthermore, colocalization was also detected between the fiber-like structures formed by CCDC102B and other linker components (LRRC45 and Cep68) (Fig. 1D), suggesting that CCDC102B belongs to the centrosome linker complex.

To visualize the detailed colocalization between CCDC102B and centrosome linker components, stimulated emission depletion (STED) nanoscopy was performed. Super-resolution images showed that, like rootletin, CCDC102B showed a clear fiber structure (Fig. 1E). The puncta of CCDC102B were adjacent to or partially overlapped

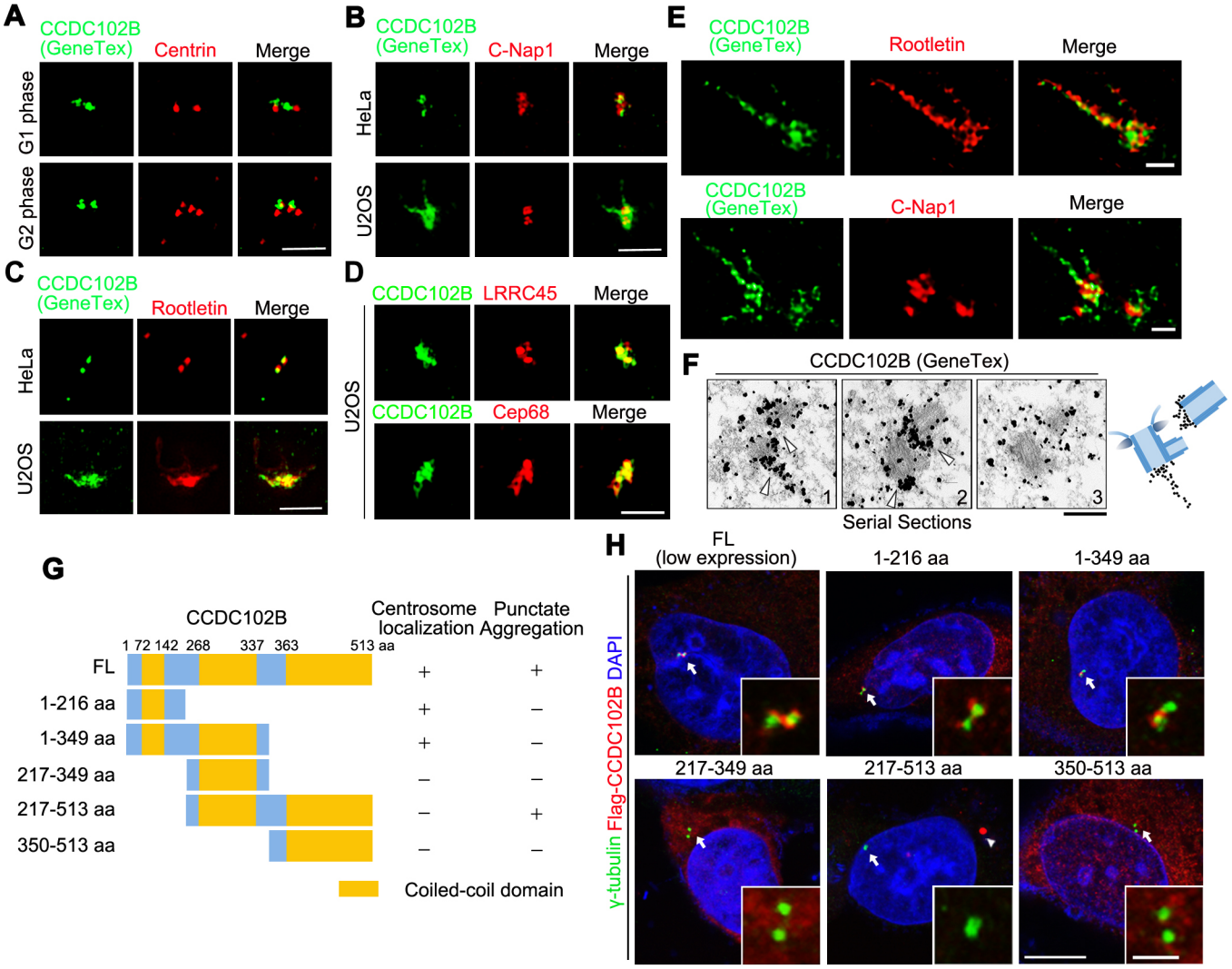

Fig. 1. CCDC102B appears as fibers at the proximal ends of centrioles. (A–C) Immunostaining of CCDC102B (green) (GeneTex antibody) and centrin (red), C-Nap1 (red) or rootletin (red) in HeLa (A–C) or U2OS (B,C) cells. Scale bars: 2 µm. (D) Immunostaining of CCDC102B (green) (in-house antibody) and LRRC45 (red) or Cep68 (red) in U2OS cells. Scale bar: 2 µm. (E) STED nanoscopy images of U2OS cells immunostained with GeneTex antibodies against CCDC102B (red) and rootletin (green) or C-Nap1 (green). Scale bars: 400 nm. (F) Immunoelectron microscopy images. U2OS cells were labeled with anti-CCDC102B antibody (GeneTex), followed by nanogold-coupled secondary antibody. A schematic of immuno-electron microscopy images is also shown on the right. Arrowheads, CCDC102B. Scale bar: 500 nm. (G) Schematic of CCDC102B full-length (FL) and truncated mutants. Coiled-coil domains, yellow; +, positive; –, negative. (H) Immunostaining of overexpressed Flag-tagged CCDC102B FL or truncated mutants (red) and γ-tubulin (green) in U2OS cells. DNA was stained with DAPI (blue). Arrows, centrosomes. Scale bars: 10 µm (main images), 2 µm (insets).

Journal of Cell Science (2018) 131, jcs222901. doi:10.1242/jcs.222901

with those of rootletin, and these two proteins formed an interdigitating network (Fig. 1E, upper panel). In addition, the CCDC102B fibers were observed to emanate from the C-Nap1 rings (Fig. 1E, lower panel). Both phenotypes were consistent with a previous observation regarding rootletin and Cep68 fibers (Vlijm et al., 2018). Immunoelectron microscopy further revealed that CCDC102B was indeed localized at the proximal ends of the centrioles and showed emanating fibers in U2OS cells with lab-generated and commercial CCDC102B antibodies (Fig. 1F; Fig. S1E,F).

We next constructed several Flag-tagged truncated mutants of CCDC102B to determine the domain that mediated its centrosome localization. Interestingly, full-length Flag–CCDC102B expressed at a low level was only localized to the centrosome, whereas, when expressed at a high level, Flag–CCDC102B formed globular aggregates in the cytoplasm (Fig. 1H; Fig. S1G). Additionally, fragments comprising 1–216 aa and 1–349 aa of CCDC102B were localized to the centrosome, while those comprising 217–349 aa and 350–513 aa were dispersed in the cytoplasm (Fig. 1G,H). Intriguingly, the fragment comprising 217–513 aa formed aggregates that were similar to those seen in the cells with expressing high levels of full-length Flag–CCDC102B (Fig. 1G,H). These results reveal that the N-terminus (1–216 aa) of CCDC102B is required for its centrosome localization, whereas the 217–513 aa region assists in the formation of globular aggregates.

Taken together, these results show that CCDC102B is enriched at the proximal ends of the centrioles and appears as fibers between them.

CCDC102B maintains centrosome cohesion

Given that CCDC102B colocalized with centrosome linker proteins (Fig. 1), we sought to examine its function in centrosome cohesion by performing siRNA-mediated depletion experiments. During interphase, centrosomes are connected tightly in U2OS cells; if the distance between the two centrosomes exceeds 2 µm, the connection is believed to be destroyed, and this process is called centrosome splitting (Mayor et al., 2000; Meraldi and Nigg, 2001; Nigg, 2006). The percentage of centrosome splitting increased from ∼6.7% in control siRNA-treated U2OS cells to ∼20.7% after the depletion of CCDC102B (Fig. 2A–C); however, it returned to ∼10.2% after overexpressing siRNA-resistant CCDC102B (Fig. 2A–C). We also measured the distance between two centrioles or centrosomes, and found that the average distance was also increased from ∼1.07 µm in control cells to ∼2.32 µm in CCDC102B-depleted cells, and it decreased to ∼1.26 µm after the reintroducing of siRNA-resistant CCDC102B (Fig. 2A,B,D). Since the centrosome linker dissolves in the G2/M transition to allow centrosome separation and bipolar spindle formation (Bahe et al., 2005; He et al., 2013; Mayor et al., 2002), some of the centrosomes that are separated in the late G2 phase might be mistakenly considered to be centrosome splitting. To exclude this possibility, we first examined whether the cell cycle progression was affected in CCDC102B-depleted U2OS cells. No significant cell cycle arrest was observed after depleting CCDC102B (Fig. S2A), suggesting that the CCDC102B depletion-induced centrosome splitting does not result from cell cycle arrest. Furthermore, we synchronized U2OS cells to G1 or G2 phases, and labeled centriole numbers by using the centriole marker centrin; ∼14.8% and 24.5% of cells showed centrosome splitting after CCDC102B depletion during G1 and G2 phases, compared with ∼5.1% and ∼10.1% in control siRNA-transfected cells, respectively (Fig. S2B,C). These data suggest that CCDC102B depletion induces centrosome splitting.

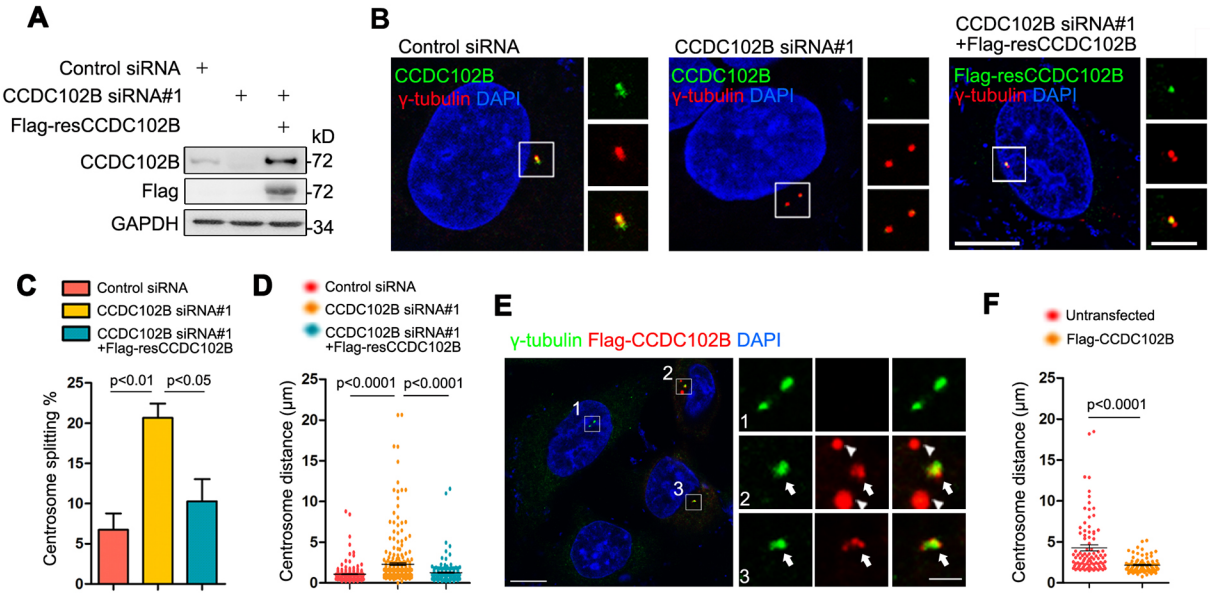

Fig. 2. CCDC102B maintains centrosome cohesion. (A) Immunoblots of CCDC102B (in-house antibody) in U2OS cells transfected with control or CCDC102B siRNA and rescued by exogenously expressing siRNA-resistant (res) CCDC102B (Flag-resCCDC102B). GAPDH was used as a loading control. (B) Immunostaining of CCDC102B (green) (in-house antibody) and γ-tubulin (red) in U2OS cells transfected with control or CCDC102B siRNA and rescued by exogenously expressing Flag–resCCDC102B (green). DNA was stained with DAPI (blue). Scale bars: 10 µm (main images), 5 µm (magnifications). (C) Quantification of the percentage of U2OS cells showing centrosome splitting from B. Centrosomes with a distance greater than 2 µm were counted as split. The siRNAs or plasmids used are as indicated. The data are presented as the mean±s.e.m. for three individual experiments with >50 cells per experiment. *P*-values are as indicated (one-way ANOVA). (D) Quantification of centrosome distance in U2OS cells from B. Each dot represents a single cell. Results are mean±s.e.m. for data pooled from three individual experiments with >50 cells per experiment. *P*-values are as indicated (one-way ANOVA). (E) Immunostaining of γ-tubulin (green) and Flag–CCDC102B (red) in Fla–CCDC102B-transfected HeLa cells. DNA was stained with DAPI (blue). Arrows, centrosome. Arrowheads, Flag–CCDC102B aggregates. Scale bars: 10 µm (main images), 2 µm (magnifications). (F) Quantification of centrosome distance in HeLa cells from E. Each dot represents a single cell. Results are mean±s.e.m. for data pooled from three individual experiments with >30 cells per experiment. *P*-values are as indicated (two-tailed Student's *t*-test).

Journal of Cell Science (2018) 131, jcs222901. doi:10.1242/jcs.222901

The centrosome connection is relatively loose in HeLa cells (Mahen, 2018). To confirm the ability of CCDC102B to maintain centrosome cohesion, we transfected Flag–CCDC102B into HeLa cells and measured the distance between two centrioles or centrosomes. Overexpressed CCDC102B not only is localized to the centrosome, but also forms globular aggregates in the cytoplasm (Fig. S1G). When measuring the distance, all the cells with centrosome-localized Flag–CCDC102B were taken into account, regardless of whether the globular aggregates existed (Fig. 2E, cell #2) or not (Fig. 2E, cell #3). The average centrosome distance decreased from ∼4.25 µm in control cells to ∼2.16 µm in cells expressing Flag–CCDC102B (Fig. 2E,F). Collectively, our results show that CCDC102B maintains centrosome cohesion during interphase.

CCDC102B is recruited to the proximal ends of the centrioles by C-Nap1

C-Nap1 provides docking sites for the localization of rootletin at the proximal ends of the centrosome and is essential for the recruitment of LRRC45 and Cep68 (Graser et al., 2007; He et al., 2013). To examine the relationship between C-Nap1 and CCDC102B, we first transfected C-Nap1–GFP into cells and found that endogenous CCDC102B was recruited to the punctate aggregates in the cytoplasm that were formed by overexpressed C-Nap1–GFP (Fig. S3A), suggesting that CCDC102B binds to C-Nap1. To investigate which domain of CCDC102B mediates its interaction with C-Nap1–GFP, we co-transfected CCDC102B truncations and C-Nap1 into U2OS cells. Similar to what was seen with full-length CCDC102B, the 1–216 aa fragment, but not the 217–513 aa fragment, of CCDC102B was colocalized with C-Nap1–GFP (Fig. 3A), suggesting that the region of 1–216 aa of CCDC102B is crucial for the interaction. In addition, immunoprecipitation assays revealed that both the N- (1–647 aa) and C-termini (1852–2442 aa) of C-Nap1 interacted with CCDC102B (Fig. 3B–D).

To determine whether the centrosome localization of CCDC102B also depends on C-Nap1, we respectively depleted CCDC102B and C-Nap1 through siRNAs in U2OS cells. The immunofluorescence images showed that the loss of C-Nap1 resulted in a decreased localization of CCDC102B at the centrosome; however, the localization of C-Nap1 was not changed upon CCDC102B depletion (Fig. 3E,F; Fig. S3B–E), suggesting that C-Nap1 acts upstream of CCDC102B. Notably, after C-Nap1 depletion, ∼77.7% of the cells showed a diminished CCDC102B signal at the centrosome, whereas ∼22.3% of the cells have long emanating CCDC102B fibers (Fig. 3E). This might be due to a minor C-Nap1 residual pool at the centrosome as previous studies shown (Bahe et al., 2005; Graser et al., 2007). Moreover, the immunoblot data showed that the protein level of CCDC102B was decreased upon C-Nap1 depletion, whereas CCDC102B depletion did not affect the protein level of C-Nap1 (Fig. S3F). Thus, C-Nap1 is required to recruit CCDC102B at the proximal ends of the centrioles.

CCDC102B associates with rootletin and LRRC45

To explore whether CCDC102B physically associates with centrosome linker proteins, we performed immunoprecipitation assays. CCDC102B co-immunoprecipitated with rootletin and LRRC45, but not with Cep68 (Fig. 4A). Overexpressing rootletin or LRRC45 alone led to the formation of large filaments in the cytoplasm (Bahe et al., 2005; He et al., 2013), to which endogenous CCDC102B was recruited (Fig. 4B), further confirming the interaction of CCDC102B with rootletin and LRRC45. However, only ∼20.7% of U2OS cells and ∼5.2% of HeLa cells expressing LRRC45–GFP showed endogenous CCDC102B recruitment to the filaments, compared with ∼98.6% of U2OS cells and ∼97.3% of HeLa cells expressing rootletin–GFP (Fig. 4B; Fig. S3G), suggesting that the interaction between LRRC45 and CCDC102B may be relatively weak and cell-type sensitive. In addition, immunoblots showed that the expression level of LRRC45–GFP was even higher than that of rootletin–GFP in both U2OS and HeLa cells (Fig. S3H), which rules out the possibility that the limited colocalization between CCDC102B and LRRC45 is due to low expression level.

To investigate which domain of rootletin is essential for CCDC102B binding, we constructed the N-terminus (1–674 aa), C-terminus (675–1340 aa) and middle region (1341–2018 aa) fragments of rootletin to perform co-immunoprecipitation assays with CCDC102B. Surprisingly, all three regions of rootletin interacted with CCDC102B (Fig. S3I,J). Similarly, both the N- (1–240 aa) and C-termini (241–670 aa) of LRRC45 interacted with CCDC102B (Fig. S3K,L). We then performed reciprocal immunoprecipitation assays to identify the regions of CCDC102B responsible for the binding of rootletin and LRRC45. The N-terminus (1–216 aa) of CCDC102B interacted with both rootletin and LRRC45 (Fig. 4C–E).

Next, we explored the recruitment relationship between CCDC102B and rootletin or LRRC45 at the centrosomes. The loss of rootletin and LRRC45 affected the recruitment of CCDC102B to the centrosome (Fig. 4F–I; Fig. S3M–P), and the total protein level of CCDC102B was also decreased after the depletion of rootletin or LRRC45 (Fig. S3F). The loss of CCDC102B also decreased the centrosome localization of rootletin and LRRC45, which was rescued after exogenously expressing siRNA-resistant Flag–CCDC102B (Fig. 4F–I; Fig. S3Q). However, the total protein level of LRRC45 remained nearly the same after CCDC102B siRNA treatment (Fig. S3F), suggesting that CCDC102B knockdown only affects the centrosome localization of LRRC45, but not its protein level.

In summary, the centrosome localization of CCDC102B depends on rootletin and LRRC45, whereas the localization of these two proteins requires CCDC102B.

CCDC102B facilitates the formation of rootletin filaments

Next, we investigated whether CCDC102B, as a centrosome linker component, is able to form filaments by self-assembly like rootletin and LRRC45 (Bahe et al., 2005; He et al., 2013; Yang et al., 2006). Overexpressing CCDC102B in cells induced the formation of globular aggregates in the cytoplasm (Figs S1G and S5A), which is different from the filament structures that are observed upon rootletin and LRRC45 overexpression (Bahe et al., 2005; He et al., 2013), suggesting that CCDC102B is not able to form filaments by self-assembly.

Rootletin or LRRC45 overexpression leads to the formation of a significant amount of intertwined large filaments in the cytoplasm. Here, we refer to these as ‘thick filaments’, while those that are nearly invisible in the cytoplasm and mainly localized at the centrosome are referred to as ‘thin filaments’. Since endogenous CCDC102B is recruited to the thick filaments of rootletin and LRRC45 in the cytoplasm (Fig. 4B), we examined whether CCDC102B affects the filament formation of rootletin and LRRC45. We first examined the filaments consisting of overexpressed LRRC45 after CCDC102B depletion using the ratio value as the metric, which is obtained by calculating the percentage of cells with thick filaments, and dividing that by the percentage of cells with thin filaments; no significant differences were detected after the loss of CCDC102B (Fig. S4B,C). However, when examining the filaments consisting of overexpressed rootletin, the ratio decreased from ∼6.6 to ∼1.7 after CCDC102B knockdown

Journal of Cell Science (2018) 131, jcs222901. doi:10.1242/jcs.222901

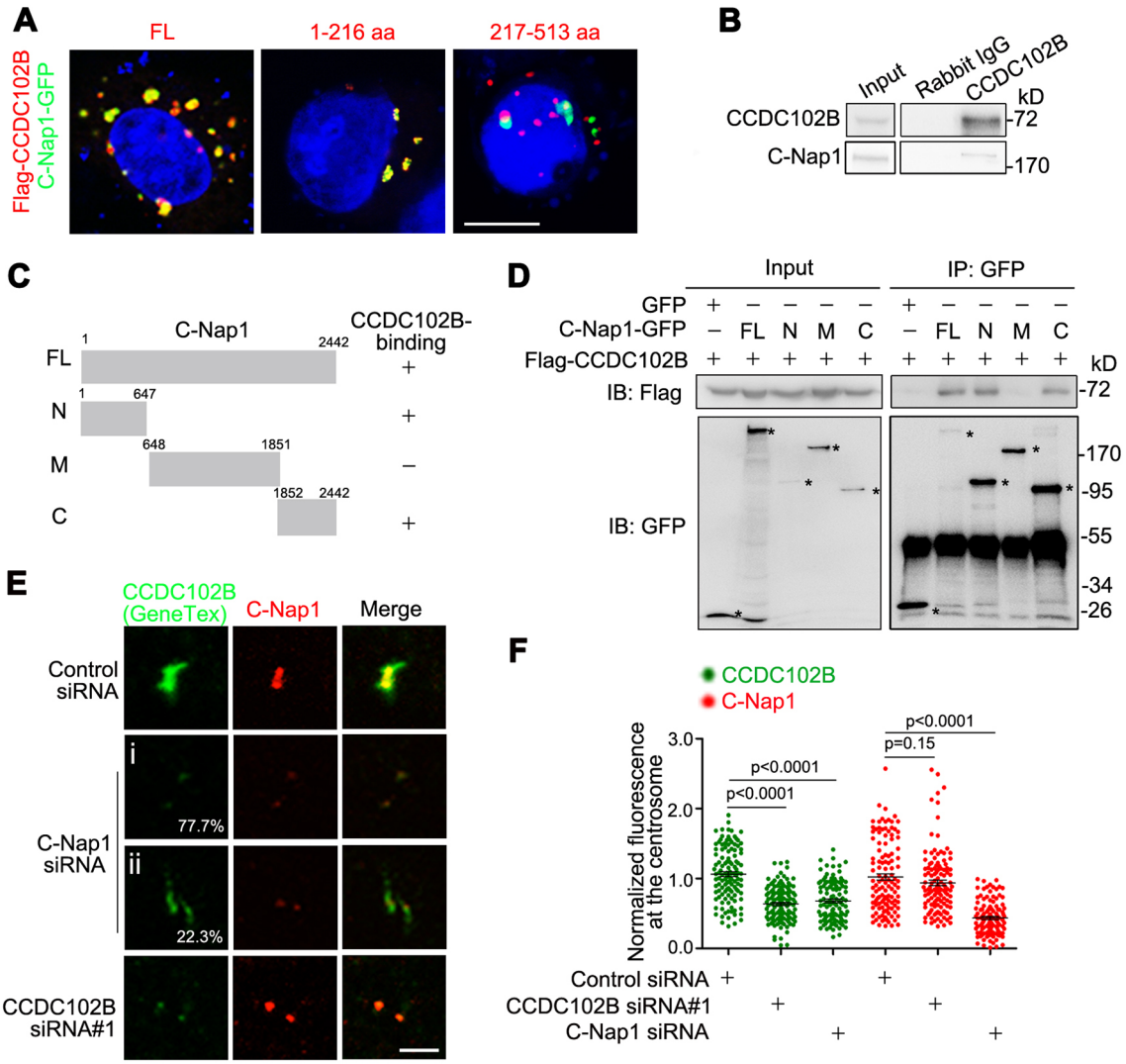

Fig. 3. CCDC102B is recruited to the centrosome through C-Nap-1. (A) U2OS cells co-overexpressing C-Nap1–GFP (green) and Flag-tagged CCDC102B full-length (FL) or truncated mutants were subjected to immunostaining with anti-Flag antibody (red). DNA was stained with DAPI (blue). Scale bar: 10 µm. (B) The anti-CCDC102B antibody (raised in-house) was used to immunoprecipitate endogenous C-Nap1 in the lysates of HEK293T cells. Antibodies used for immunoblots (IB) are as indicated. (C) Schematic of C-Nap1 FL and its truncated mutants (denoted N, M and C). +, positive; –, negative. (D) Lysates of HEK293T cells overexpressing Flag-tagged CCDC102B and the indicated GFP-tagged FL or truncated mutants of C-Nap1 were subjected to immunoprecipitation (IP) and IB, as indicated. *, indicates expected bands. (E) Immunostaining of CCDC102B (green) (GeneTex antibody) and C-Nap1 (red) in U2OS cells transfected with control siRNA, C-Nap1 siRNA or CCDC102B siRNA. The percentage on the i and ii panel for C-Nap1 siRNA indicates the percentage of C-Nap1-depleted cells. Scale bar: 2 µm. (F) Quantitative analysis of the fluorescence intensity of CCDC102B and C-Nap1 at the centrosome from E. Each dot represents a single cell. Results are mean±s.e.m. for data pooled from three individual experiments with >40 cells per experiment. *P*-values are as indicated (one-way ANOVA).

(Fig. 5A,B). Similarly, the loss of Cep68 also led to a decrease of the ratio (~2.0) (Fig. 5A,B), which is consistent with a previous study (Vlijm et al., 2018). Furthermore, the ratio did not decrease significantly in CCDC102B/Cep68 double-knockdown cells (~2.1) compared with those from single-knockdown cells (Fig. 5A,B). Immunoblots showed that the expression level of rootletin remained almost the same after the treatment of CCDC102B- or Cep68-siRNA, suggesting that the change in the filament formation of rootletin–GFP is not due to altered expression of the proteins (Fig. 5C). In addition, the ratio returned to ~4.6 after reintroducing siRNA-resistant CCDC102B, but not Cep68 (~2.0) (Fig. 5A,B). Overexpressing CCDC102B in Cep68-knockdown cells did not significantly affect the ratio (~1.6) (Fig. 5A,B). Taken together, both CCDC102B and Cep68 contribute to the filament formation of rootletin, while CCDC102B cannot rescue the effect of Cep68 depletion on rootletin filament formation, or vice versa.

We next examined the recruitment relationship between CCDC102B and Cep68 at the centrosome. The loss of CCDC102B did not significantly affect the fluorescence intensity of Cep68 at the centrosome, or vice versa (Fig. S4D,E). In general, except for the fiber-like structures of CCDC102B at the centrosome, CCDC102B appeared as dot-like structures in some cells (Fig. S4D). We calculated the percentage of cells with fiber-like structures, and divided that by the percentage of cells with dot-like structures to obtain a ratio value. The results showed that the ratio decreased from ~2.6 in control cells to ~0.7 in Cep68-depleted cells (Fig. S4D,F). These results suggest that Cep68 does not affect the centrosome localization of CCDC102B but is essential for the fiber structure formation of CCDC102B.

In conclusion, CCDC102B does not form filaments through self-assembly but is recruited to the filaments of rootletin, and together with Cep68, it facilitates the filament formation of rootletin.

Journal of Cell Science (2018) 131, jcs222901. doi:10.1242/jcs.222901

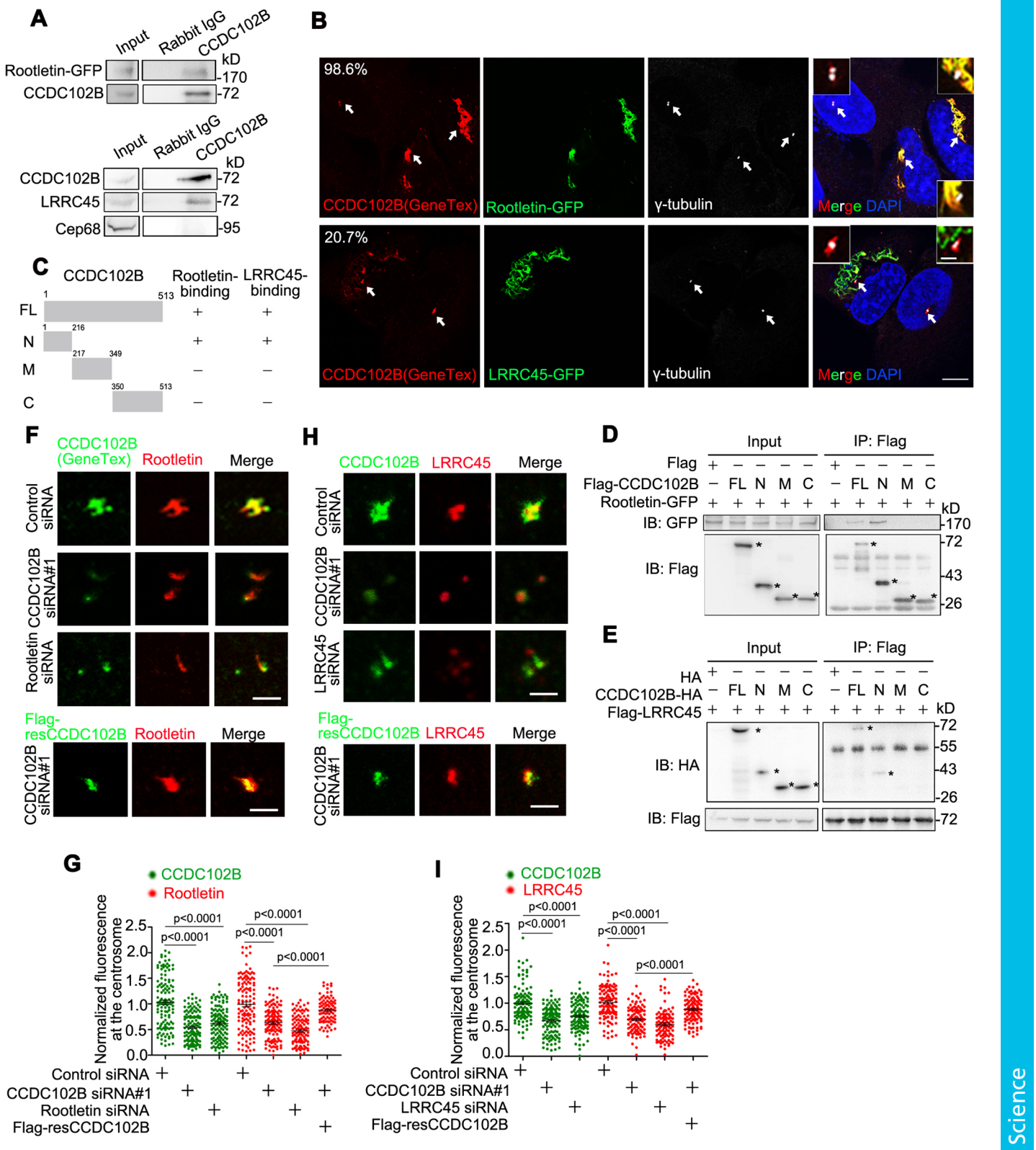

Fig. 4. See next page for legend.

CCDC102B is dissociated from the centrosome by Nek2A-mediated phosphorylation

C-Nap1, rootletin and LRRC45 are phosphorylated by Nek2A, a cell cycle-regulated kinase that is enriched at the centrosome, and are dissociated from the centrosomes during mitosis (Bahe et al., 2005; Fry et al., 1998; He et al., 2013; Man et al., 2015; Mayor et al., 2002; Yang et al., 2006). We observed that the localization of CCDC102B at the centrosome became weak when cells entered prophase and was significantly decreased in metaphase (Fig. 6A,B; Fig. S5A,B). These data prompted us to test whether the removal of

Journal of Cell Science (2018) 131, jcs222901. doi:10.1242/jcs.222901

Fig. 4. CCDC102B is associated with rootletin and LRRC45. (A) The anti-CCDC102B antibody (raised in-house) was used to immunoprecipitate exogenously expressed rootletin–GFP (upper panel) and endogenous LRRC45 and Cep68 (lower panel) in lysates of HEK293T cells. The antibodies used for immunoblots (IB) are as indicated. (B) Immunostaining of CCDC102B (red; GeneTex antibody) and γ-tubulin (white) in U2OS cells transfected with rootletin–GFP (green) or LRRC45–GFP (green). DNA was stained with DAPI (blue). The percentage indicates the percentage of cells in which endogenous CCDC102B was recruited to the filaments of rootletin–GFP or LRRC45–GFP. Scale bars: 10 µm (main images); 2 µm (magnified centrosomes). Arrows, centrosomes. (C) Schematic of CCDC102B full-length (FL) and its truncated mutants (denoted N, M and C). +, positive; –, negative. (D) Lysates of HEK293T cells overexpressing rootletin–GFP and the indicated Flag-tagged FL or truncated mutants of CCDC102B were subjected to immunoprecipitation (IP) and IB, as indicated. *, indicates expected bands. (E) Lysates of HEK293T cells overexpressing Flag–LRRC45 and the indicated HA-tagged FL or truncated mutants of CCDC102B were subjected to IP and IB, as indicated. *, indicates expected bands. (F) Immunostaining of CCDC102B (green; GeneTex antibody) or siRNA-resistant (res) CCDC102B (Flag-resCCDC102B) (green) and rootletin (red) in U2OS cells transfected with control siRNA, CCDC102B siRNA or rootletin siRNA. Scale bar: 2 µm. (G) Quantitative analysis of the fluorescence intensity of CCDC102B and rootletin at the centrosome from F. Each dot represents a single cell. Results are mean±s.e.m. from data pooled from three individual experiments with >40 cells per experiment. *P*-values are as indicated (one-way ANOVA). (H) Immunostaining of CCDC102B (green; in-house antibody) or Flag-resCCDC102B (green) and LRRC45 (red) in U2OS cells transfected with control siRNA, CCDC102B siRNA or LRRC45 siRNA. Scale bar: 2 µm. (I) Quantitative analysis of the fluorescence intensity of CCDC102B and LRRC45 at the centrosome from H. Each dot represents a single cell. Results are mean±s.e.m. from data pooled from three individual experiments with >40 cells per experiment. *P*-values are as indicated (one-way ANOVA).

CCDC102B from the centrosome upon mitosis is also mediated by Nek2A-dependent phosphorylation. Upshifted Flag–CCDC102B bands were detected in the samples of mitosis-arrested cells but not those of interphase cells, whereas upshifted bands were hardly detected after treatment with lambda protein phosphatase (λ-PPase) (Fig. S5C), indicating that CCDC102B is phosphorylated during mitosis.

To further investigate whether CCDC102B is a substrate of Nek2A, we first conducted a co-immunoprecipitation experiment and found that Nek2A interacted with the N-terminus (1–216 aa) of CCDC102B (Fig. S5D). We then co-overexpressed GFP-tagged wild-type Nek2A (Nek2A-WT–GFP) or the catalytically inactive (kinase-dead) mutant Nek2A (Nek2A-K37R–GFP) (Fry, 2002; Hames and Fry, 2002) with Flag–CCDC102B in HeLa cells (Fig. 6C). The resulting immunoblots showed obvious, smeared, upshifted bands of Flag–CCDC102B when it was co-overexpressed with Nek2A-WT–GFP but not with Nek2A-K37R–GFP (Fig. 6C), suggesting that Nek2A phosphorylates CCDC102B. By applying mass spectrometry analysis, ten different phosphorylation sites of CCDC102B (S21, S22, S34, S135, S142, S194, S210, S401, S404, and S406) were identified in the cells co-overexpressing Nek2A-WT that were not present in cells with Nek2A-K37R (Fig. S5E). Next, we generated a non-phosphorylatable mutant of CCDC102B in which all of the ten serine residues were mutated to alanine residues (CCDC102B-10A). The upshifted smeared bands of CCDC102B-10A were substantially decreased compared with those of CCDC102B-WT when cells were co-overexpressed with Nek2A-WT, whereas a clear shift compared with control was observed (Fig. 6C), implying that Nek2A also phosphorylates CCDC102B at other sites. To further validate whether Nek2A phosphorylates CCDC102B at the onset of mitosis, we overexpressed CCDC102B-WT or the CCDC102B-10A mutant in HeLa cells and synchronized the cells to the G2/M phase with nocodazole treatment. The amount of the upshifted bands of CCDC102B was much less in cells expressing the 10A mutant compared to the WT cells (Fig. 6D).

Next, we determined whether the displacement of CCDC102B from the centrosome is induced by Nek2A-mediated phosphorylation. The centrosome localization of Flag–CCDC102B was markedly decreased in interphase cells when co-overexpressed with Nek2A-WT–GFP but not with the Nek2A-K37R–GFP mutant (Fig. 6E,F). Additionally, the CCDC102B-10A mutant was not displaced from the centrosome in the presence of WT Nek2A (Fig. 6E,F). Moreover, similar to C-Nap1 (Fig. S5F–H) (Fry, 2002; He et al., 2013), the removal of CCDC102B from the centrosomes was blocked in Nek2A-depleted mitotic cells (Fig. 6G,H; Fig. S5G,H). Taken together, these results show that CCDC102B is removed from the centrosome after phosphorylation, which is regulated by Nek2A.

DISCUSSION

In our study, we found that CCDC102B participates in the assembly of the centrosome linker and cooperates with other linker proteins to maintain centrosome tethering (Fig. 7). In interphase, CCDC102B appears as fibers at the proximal ends of centrioles. At the onset of mitosis, along with other centrosome components, CCDC102B is phosphorylated by Nek2A and is disassociated from the centrosome to allow for the centrosome separation (Fig. 7A).

The loss of either CCDC102B or Cep68 affects the filament formation of overexpressed rootletin (Fig. 5A); one possibility for this is that these two proteins function independently in regulating the formation of rootletin filaments. However, since CCDC102B/Cep68 double-knockdown did not further decrease the ratio compared with that seen with either CCDC102B or Cep68 single knockdown (Fig. 5A,B), and considering that Cep68 is required for the fiber structure formation of endogenous CCDC102B, we proposed the model shown in Fig. 7B. Rootletin forms thin filaments through self-assembly, whereas CCDC102B and Cep68 do not form filaments on their own (Fig. S4A) (Graser et al., 2007) but are recruited to the filaments of rootletin sequentially. These two proteins then facilitate the formation of thick rootletin filaments (Fig. 7B). The loss of Cep68 affects the fiber structures instead of the centrosome fluorescence intensity of endogenous CCDC102B (Fig. S4D–F), probably because without Cep68, CCDC102B only attaches to the short fibers around the proximal ends of the centrioles, but not to the emanating long fibers formed by rootletin (Vlijm et al., 2018). However, no interaction between CCDC102B and Cep68 could be detected via immunoprecipitation (Fig. 4A), which may be due to the small amounts of the endogenous proteins or because there is an unknown protein mediating the interaction between them.

CCDC102B is localized to the centrosome mainly through its N-terminus (1–216 aa), and this domain is also crucial for interacting with C-Nap1, rootletin and LRRC45 (Fig. 7C). C-Nap1 forms ring-like structures at the proximal ends of the centrioles (Fig. 1E) (Vlijm et al., 2018) and acts upstream of rootletin, LRRC45, Cep68 and CCDC102B (Fig. 3) (Bahe et al., 2005; Graser et al., 2007; He et al., 2013). It is possible that CCDC102B is recruited to the centrosome primarily by rootletin and interacts with C-Nap1 indirectly through rootletin.

LRRC45 interacts with CCDC102B and affects its centrosome localization and vice versa (Fig. 4E,H). However, CCDC102B knockdown does not affect the cytoplasmic filaments formed from overexpressed LRRC45 (Fig. S4B,C). Thus, CCDC102B may not directly interact with LRRC45, and it may only affect the centrosome localization, and not the filament assembly function, of LRRC45.

Our results show that C-Nap1, rootletin and LRRC45 are all responsible for the recruitment of CCDC102B to the centrosome,

Journal of Cell Science (2018) 131, jcs222901. doi:10.1242/jcs.222901

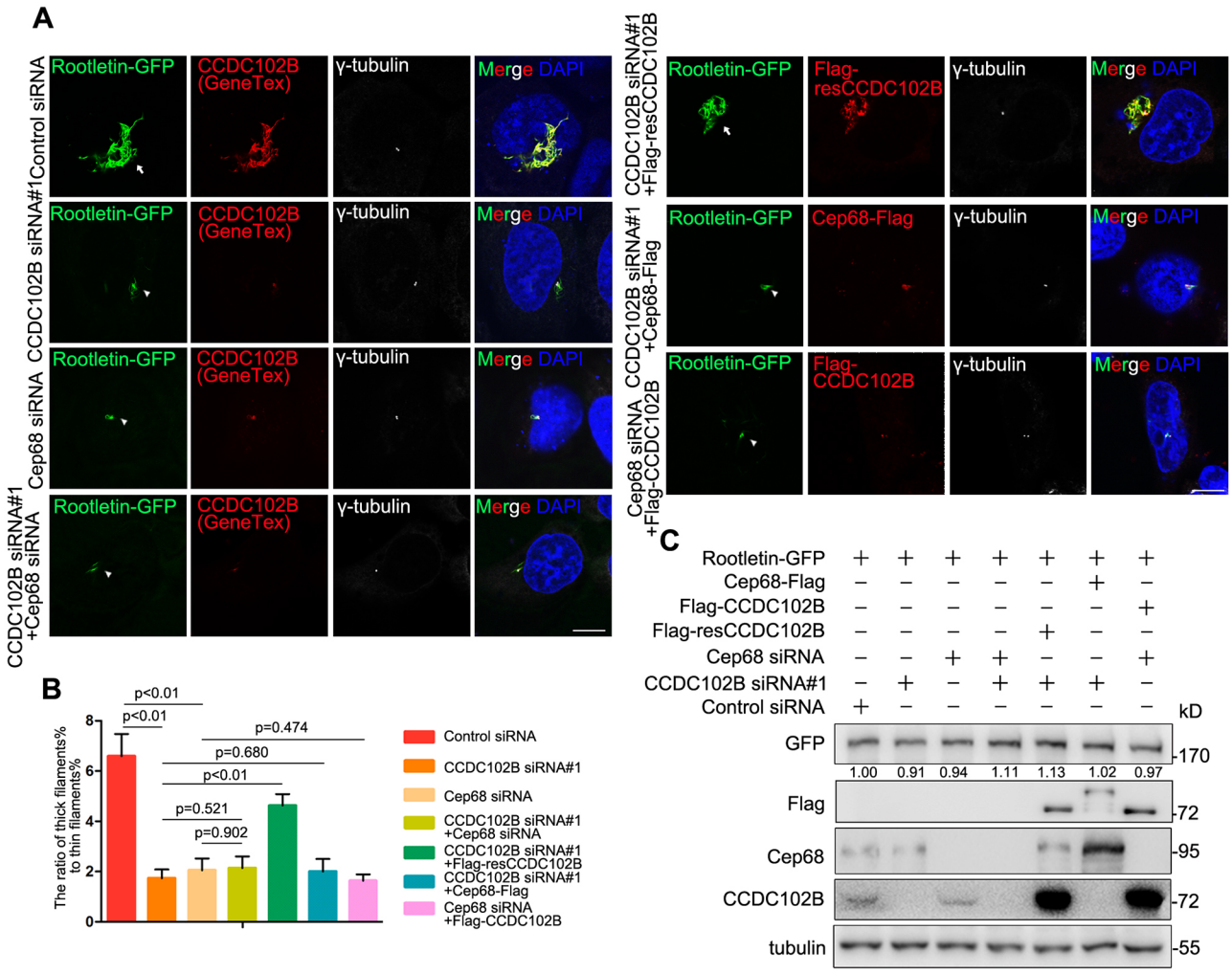

Fig. 5. CCDC102B facilitates the formation of rootletin filaments. (A) Immunostaining of endogenous CCDC102B (red; GeneTex antibody) and γ-tubulin (white) in U2OS cells transfected with rootletin–GFP (green) and the indicated siRNAs or together with siRNA-resistant CCDC102B (Flag-resCCDC102B) (red), Flag–CCDC102B (red) or Cep68–Flag (red). After siRNA treatment for 24 h, the cells were transfected with rootletin–GFP (green) and the indicated proteins (red) for an additional 48 h. DNA was stained with DAPI (blue). Arrows, rootletin–GFP thick filaments. Arrowheads, rootletin–GFP thin filaments. Scale bars: 10 µm. (B) Quantification of the ratio value, which is obtained by calculating the percentage of cells with rootletin thick filaments, and dividing that by the percentage of cells with rootletin thin filaments, from A. Results are mean±s.e.m. from three individual experiments with >100 cells per experiment. *P*-values are as indicated (one-way ANOVA). (C) Lysates of U2OS cells from A were subjected to immunoblotting. Tubulin is used as a loading control. Relative amounts of rootletin–GFP were quantified and normalized to tubulin. Three individual experiments were performed, and results from a representative experiment are shown.

while CCDC102B contributes to the centrosome localization of rootletin and LRRC45. All of these linker proteins are disassociated from the centrosome at the onset of mitosis after the phosphorylation mediated by Nek2A (Bahe et al., 2005; He et al., 2013; Mayor et al., 2002). However, the reduction of CCDC102B at the centrosome appears to be much less than that seen with other linker proteins like C-Nap1 and rootletin (Fig. 6A; Fig. S5A). Thus, whether the centrosome localization of CCDC102B is under the regulation of Nek2A-independent pathways or proteins and whether they contribute to the recruitment of overexpressed CCDC102B-10A to the centrosome regardless of Nek2A overexpression (Fig. 6E) require further study.

Although the centrosome localization of the centrosome linker components decreased during mitosis, the detailed mechanisms seem to not exactly be the same. Cep68 is degraded in prometaphase through the action of the $SCF^{\beta TcCP}$ ubiquitin ligase complex (Man et al., 2015; Pagan et al., 2015). The protein levels of C-Nap1 and LRRC45 are decreased in mitosis through an unknown mechanism (He et al., 2013; Mayor et al., 2002). Surprisingly, the protein level of CCDC102B was elevated during mitosis, which is similar to what is found for rootletin (Mahen, 2018), indicating that a unique pathway to balance the protein level and centrosome localization of these proteins should exist. Further study will also focus on how the linker components hierarchically dissemble from centrosomes through different pathways.

A recent study has reported that LRRC45 and Cep68 are required for cilia formation (Loukil et al., 2017). Moreover, CCDC88, a protein that has a high level of similarity to CCDC102B (Hosoda et al., 2018), is colocalized with C-Nap1 and regulates basal body localization and ciliogenesis via rootletin in human RPE-1 cells (Nechipurenko et al., 2016). Future studies will be focused on the relationship between centrosome tethering and ciliogenesis.

MATERIALS AND METHODS

Plasmid construction

Human CCDC102B (NM_001093729.1) and its mutants were amplified by PCR and cloned into pEGFP-N3 (Clontech Laboratories), pcDNA3.1-HA

Journal of Cell Science (2018) 131, jcs222901. doi:10.1242/jcs.222901

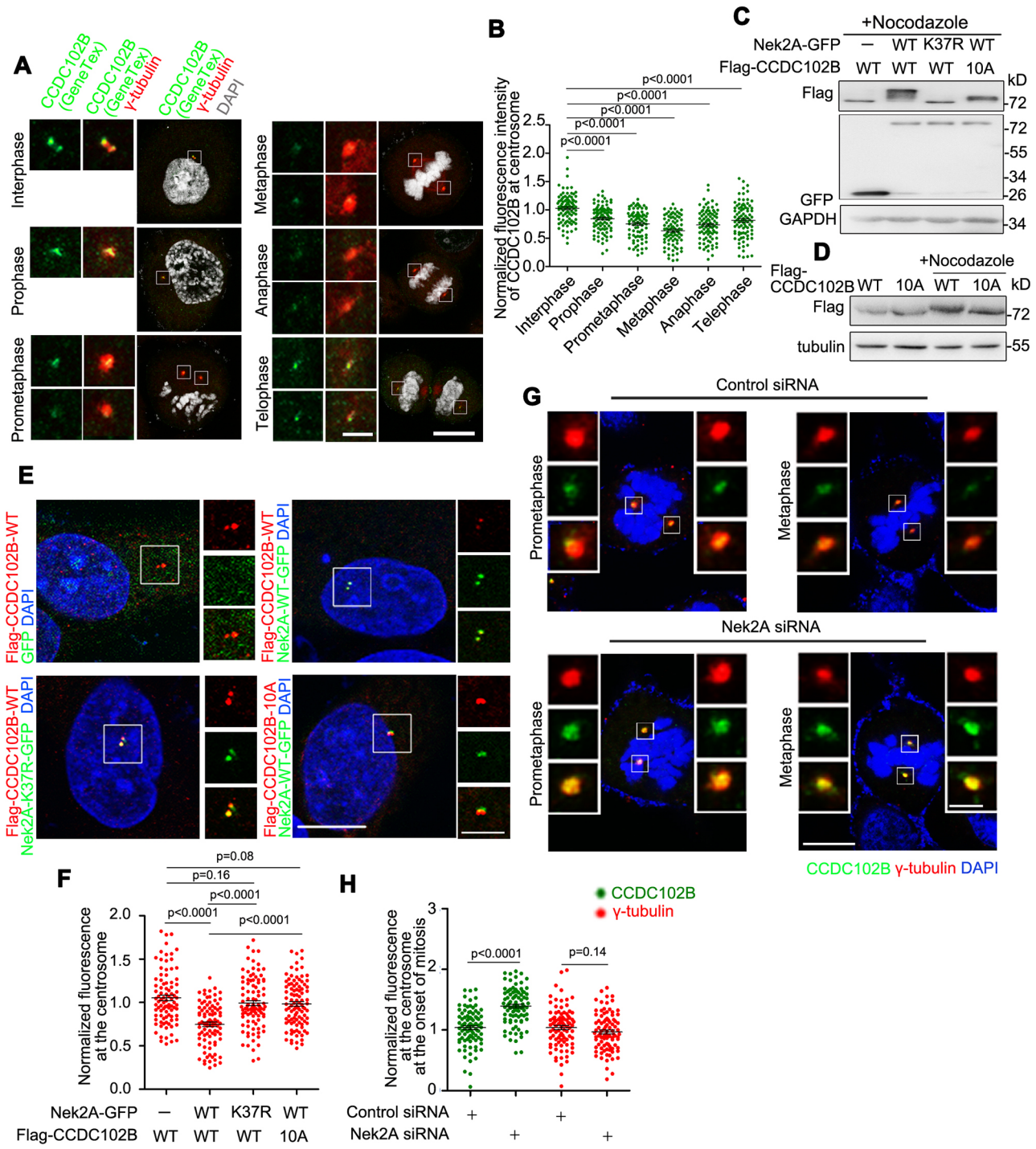

Fig. 6. See next page for legend.

and p3×Flag-CMV-7.1 (Sigma-Aldrich). Human LRRC45 (He et al., 2013) (NM_144999) was amplified by PCR and cloned into pEGFP-N3 (Clontech Laboratories) and p3×Flag-CMV-7.1 (Sigma-Aldrich). Human Cep68 (NM_015147.2) was amplified by PCR and cloned into p3×Flag-CMV-14 (Sigma-Aldrich). Rootletin was PCR-amplified from pACT2-Rootletin provided by Erich A. Nigg (University of Basel, Basel, Switzerland) (Bahe et al., 2005) and cloned into pEGFP-C1 (Clontech Laboratories). Nek2A wild-type and K37R were PCR amplified from pEGFP-Nek2A, which was provided by Andrew M. Fry (University of Leicester, Leicester, UK) (Fry et al., 1998). pEGFP-C-Nap1 was provided by Kunsoo Rhee (Seoul National University, Seoul) (Kim et al., 2008).

Antibodies

The primary antibodies used were against CCDC102B [1:200 for immunoblotting (IB) and immunofluorescence (IF); mouse; generated in-house], CCDC102B (1:500 for IB and 1:100 for IF; rabbit; GTX107182; GeneTex), LRRC45 (1:1000 for IB and 1:200 for IF; rabbit; HPA024768; Sigma-Aldrich), rootletin (1:200 for IF; mouse; SC-374056; Santa Cruz Biotechnology), C-Nap1 (1:100 for IB and IF; mouse; SC-135851; Santa Cruz Biotechnology), Cep68 (1:500 for IB and 1:100 for IF; rabbit; 15147-1-AP; Proteintech), Nek2 (1:2000 for IB and 1:200 for IF; mouse; 610593; BD Transduction), centrin-3 (1:200 for IF; mouse; ABIN2966513; Abnova), cyclin B (1:1000 for IB; rabbit; 4138; Cell Signaling), α-tubulin

Journal of Cell Science (2018) 131, jcs222901. doi:10.1242/jcs.222901

Fig. 6. CCDC102B is dissociated from the centrosome after being phosphorylated by Nek2A. (A) Immunofluorescence analysis of CCDC102B (green; Genetex antibody) and γ-tubulin (red) in HeLa cells. DNA was stained with DAPI (white). Scale bars: 10 µm (main images); 5 µm (magnified centrosomes). (B) Quantitative analysis of CCDC102B fluorescence intensity at the centrosome from A. Each dot represents a single cell. Results are mean±s.e.m. for data pooled from three individual experiments with >30 cells per experiment. *P*-values are as indicated (one-way ANOVA). (C) Lysates of Flag-tagged CCDC102B-wild-type (WT) or CCDC102B-10A (S21A, S22A, S34A, S135A, S142A, S194A, S210A, S401A, S404A, and S406A)-overexpressing U2OS cells co-transfected with GFP-tagged Nek2A-WT or its kinase-dead mutant (Nek2A-K37R) were immunoblotted using anti-Flag antibodies. The cells were arrested at G2/M phase with nocodazole treatment for 24 h. GAPDH was used as a loading control. (D) HeLa cells overexpressing Flag-tagged CCDC102B-WT or CCDC102B-10A were arrested at G2/M phase with nocodazole treatment for 24 h. The lysates were subjected to immunoblotting using phos-tag gels. GAPDH was used as a loading control. (E) Fluorescence images of Flag-tagged CCDC102B-WT (red) or CCDC102B-10A (red) overexpressed in U2OS cells after co-transfection with GFP-tagged Nek2A-WT (green) or Nek2A-K37R (green). DNA was stained with DAPI (blue). Scale bars: 10 µm (main images); 5 µm (magnified centrosomes). (F) Quantification of the fluorescence intensity of CCDC102B at the centrosome from E. Each dot represents a single cell. Results are mean ±s.e.m. for data pooled from three individual experiments with >30 cells per experiment. *P*-values are as indicated (one-way ANOVA). (G) Immunostaining of CCDC102B (green; in-house antibody) and γ-tubulin (red) in synchronized U2OS cells after transfection with control siRNA or Nek2A siRNA. DNA was stained with DAPI (blue). Scale bars: 10 µm (main images); 5 µm (magnified centrosomes). (H) Quantification of the fluorescence intensities at the centrosomes from G. Each dot represents a single cell. Results are mean ±s.e.m. for data pooled from three individual experiments with >30 cells per experiment. *P*-values are as indicated (two-tailed Student's *t*-test).

(1:1000 for IB; mouse; T9026; Sigma-Aldrich), γ-tubulin (1:1000 for IB and 1:200 for IF; mouse; T6557; Sigma-Aldrich), γ-tubulin (1:200 for IF; rabbit; T3559; Sigma-Aldrich), GAPDH (1:2000 for IB; mouse; CW0101M; CWBIO), HA (1:2000 for IB; mouse; H9658; Sigma-Aldrich), Flag (1:2000 for IB and 1:200 for IF; mouse; F1804; Sigma-Aldrich) and GFP (1:5000 for IB; rabbit; generated in-house). The secondary antibodies Alexa Fluor 488/568/647-conjugated goat anti-mouse/rabbit IgG (1:200; Invitrogen) and horseradish peroxidase (HRP)-cojugated goat anti-mouse/rabbit IgG (1:5000; Jackson ImmunoResearch) were also used.

Cell culture, transfection, and cell synchronization

HeLa and HEK293T cells were obtained from the American Type Culture Collection. U2OS cells were provided by Xueliang Zhu (SIBS, Chinese Academy of Sciences, Shanghai, China) (Cao et al., 2012; Zhao et al., 2013). All cells were cultured in DMEM (GIBCO) supplemented with 10% fetal bovine serum (CellMax). The cells were transfected with jetPEI (Polyplus transfection) or Lipofectamine™ 2000 (Invitrogen) according to the manufacturer's instructions.

For low and high expression, the cells were transfected with the indicated plasmid for 16 h and 32 h, respectively.

To arrest the cell in G2/M phase, HeLa cells were treated with 100 ng/ml nocodazole for 24 h. For the double-thymidine blocking, HeLa cells were treated with 2.5 mM thymidine for 24 h, released for 12 h, and blocked again for 24 h.

Gene silencing by siRNA

All siRNAs were obtained from Invitrogen; the sequences used in this study are as follows: CCDC102B#1, 5′-GCUGAGACUGAAAGCAAUA-3′; CCDC102B#2, 5′-GGACAAGAGGGAAAUACUU-3′; C-Nap1, 5′-UUCUCCGAACGUGUCACGU-3′ (He et al., 2013); rootletin, 5′-AAGCCAGTCTAGACAAGGA-3′ (Bahe et al., 2005); LRRC45, 5′-CCAACAGAACAAGUCCAUU-3′ (He et al., 2013); Cep68, 5′-CGAAGAUGAUCCAUCCCUA-3′; Nek2A, 5′-AAACAUCGUUCGUUACUAU-3′ (He et al., 2013) and scrambled control siRNA, 5′-UUCUCCGAACGUGUGUCACGU-3′.

To generate siRNA-resistant CCDC102B (resCCDC102B), six silent mutations were introduced into the CCDC102B sequence by PCR amplification (5′-GCTGAGACTGAAAGCAATA-3′ mutated to 5′-GCAGAAACGGAGAGTAACA-3′; 5′-GGACAAGAGGGAAATACTT-3′ mutated to 5′-GGATAAAAGAGAGATTCTG-3′).

All siRNAs were transfected using Lipofectamine 2000 RNAi transfection reagent (Invitrogen) at a final concentration of 50 nM according to the manufacturer's instructions, and cells were analyzed 72 h after transfection. For the rescue assay, after the treatment of siRNA for 24 h, cells were transfected with resCCDC102B for an additional 48 h and subjected to further analysis.

Immunofluorescence and electron microscopy

For immunofluorescence, the cells were fixed and permeabilized in cold methanol for 7–10 min at −20°C. The cells were then incubated with primary antibodies at 4°C overnight and secondary antibodies at room

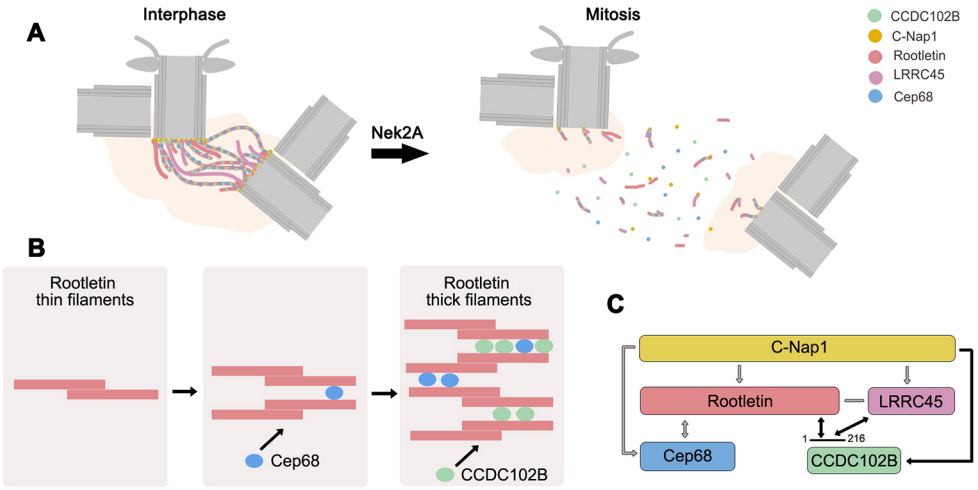

Fig. 7. Schematic model for the role of CCDC102B in centrosome linker assembly. (A) In interphase, CCDC102B appears as fibers at the proximal ends of the centrioles. In mitosis, CCDC102B and other linker components are phosphorylated by Nek2A and dissociate from the centrosome to initiate centrosome separation. (B) Schematic of the role of CCDC102B and Cep68 in facilitating the formation of thick rootletin filaments. (C) C-Nap1 acts upstream of rootletin (Bahe et al., 2005; Yang et al., 2006), LRRC45 (He et al., 2013), Cep68 (Graser et al., 2007) and CCDC102B. CCDC102B interacts with rootletin and LRRC45 through its 1–216 aa sequence. The centrosome localization between CCDC102B and rootletin or LRRC45 is interdependent. Gray line, interaction identified by previous reports (Graser et al., 2007; He et al., 2013; Yang et al., 2006). Black line, interaction identified here. The directions of the arrow indicate recruitment relationships.

temperature for 1 h, sequentially. Next, the cells were stained with 1 µg/ml 4,6-diamidino-2-phenylindole (DAPI). The samples were observed at room temperature using a fluorescence microscope (TH4-200, Olympus) equipped with a 60×1.42 NA apo oil objective lens (Olympus). Confocal microscopy and STED nanoscopy were performed using a confocal microscope (TCS SP8, Leica) equipped with a 100×1.4 NA apo oil objective lens. The images were acquired with LAS X software (Leica). STED nanoscopy image deconvolution was carried out by Huygens software (Scientific Volume Imaging, The Netherlands). Three-dimensional structured illumination microscopy (3D-SIM) was performed using the N-SIM System (Nikon) with a 100×1.49 NA apo oil objective lens (Nikon). The images were acquired by NIS-Elements AR software (Nikon) after being reconstructed to maximum projections. All images were processed in Photoshop (CS5; Adobe).

For the immunoelectron microscopy, U2OS cells were fixed with 4% paraformaldehyde (PFA) in PBS for 10 min at room temperature, followed by 0.5% Triton X-100 for 3 min. The cells were then incubated with primary antibodies (anti-CCDC102B, 1:10, Genetex; 1:20, made in-house) in phosphate buffer (0.1 M Na_2HPO_4, 0.2 M NaH_2PO_4; pH 7.4) at 4°C overnight and secondary antibodies (goat anti-rabbit IgG-nanogold antibody, 1:50, Nanoprobes) at room temperature for 60 min, sequentially. HQ Silver (Nanoprobes) was used to enhance the nanogold signal for ∼12 min. The samples were postfixed in 1% osmium tetroxide in phosphate buffer for 30 min and stained with 1.5% uranyl acetate (in 50% ethanol) for 30 min on ice. Next, the samples were dehydrated and embedded in Epon. Finally, after staining with 3% aqueous uranyl acetate and 0.4% lead citrate, the sections were imaged with a transmission electron microscope (FEI, Tecnai G2 20 Twin).

Immunoprecipitation and immunoblots

For immunoprecipitation, HEK293T cells were washed three times using cold PBS and lysed in immunoprecipitation lysis buffer (50 mM HEPES, 0.1% NP-40, 250 mM NaCl, 1 mM DTT, 5 mM EDTA, 10% glycerol, protease inhibitors; pH 7.5) on ice for 30 min after transfection for 36–48 h. Appropriate antibodies, protein G–Sepharose or protein A–Sepharose beads (Amersham Biosciences) and the supernatants of the lysates were incubated for 2 h after the lysates were centrifuged at 20,000 ***g*** for 15 min at 4°C. After washing with the lysis buffer four times, the beads were collected and boiled at 100°C for 5 min in SDS loading buffer. For the λ-PPase treatment, the cell lysates were treated with λ-PPase (NEB) for 30 min according to the manufacturer's instructions.

For immunoblotting, the samples were resolved by SDS-PAGE and transferred to a PVDF membrane (Millipore). The membrane was incubated with primary antibodies and HRP-conjugated secondary antibodies, sequentially. For the separation of phosphorylated substances, Phos-tag gels (Wako) were used.

Flow cytometry analysis

The cells were trypsinized and centrifuged at 1000 ***g*** for 3 min. After washing two times with PBS, the cells were fixed in cold 70% ethanol (added dropwise) for 30 min. The cells were then washed with PBS and incubated with 100 mg/ml RNase A in PBS for 20 min at 37°C. Finally, the cells were incubated with 10 mg/ml propidium iodide (PI) on ice for 30 min and analyzed using FACScalibur (BD Biosciences) and CellQuest software.

Measurements and statistical analysis

The fluorescence intensity and the distance between two centrosomes were measured using ImageJ software (NIH). All experiments were individually performed at least three times.

Acknowledgements

We thank Erich A. Nigg (University of Basel, Basel, Switzerland), A. M. Fry (University of Leicester, Leicester), and K. Rhee (Seoul National University, Seoul) for the reagents; Chunyan Shan and Xiaochen Li (the Core Facilities of Life Sciences, Peking University) for the 3D-SIM and confocal microscopy imaging; and Liying Du and Hongxia Lu (the Core Facilities of Life Sciences, Peking University) for the flow cytometry and statistical analysis. We thank all members of the laboratory for their helpful discussions.

Competing interests

The authors declare no competing or financial interests.

Author contributions

Conceptualization: Y.X., N.H.; Methodology: Y.X., N.H., Z.C., F.L., G.F., D.M.; Software: Y.X.; Validation: Y.X.; Formal analysis: Y.X., N.H.; Investigation: Y.X., N.H.; Resources: Y.X., J.T., J.C.; Data curation: Y.X.; Writing - original draft: Y.X.; Writing - review & editing: Y.X., N.H., J.T., J.C.; Visualization: Y.X., N.H.; Supervision: J.T., J.C.; Project administration: Y.X.; Funding acquisition: J.T., J.C., D.M.

Funding

This work was supported by the National Natural Science Foundation of China (31830110, 31801133, 31571376 and 31471280) and the National Key Research and Development Program of China, Stem Cell and Translational Research (2016YFA0100501).

Supplementary information

Supplementary information available online at http://jcs.biologists.org/lookup/doi/10.1242/jcs.222901.supplemental

References

Au, F. K. C., Jia, Y., Jiang, K., Grigoriev, I., Hau, B. K. T., Shen, Y. H., Du, S. W., Akhmanova, A. and Qi, R. Z. (2017). GAS2L1 is a centriole-associated protein required for centrosome dynamics and disjunction. *Dev. Cell* **40**, 81-94.

Bahe, S., Stierhof, Y.-D., Wilkinson, C. J., Leiss, F. and Nigg, E. A. (2005). Rootletin forms centriole-associated filaments and functions in centrosome cohesion. *J. Cell Biol.* **171**, 27-33.

Bahmanyar, S., Kaplan, D. D., DeLuca, J. G., Giddings, T. H., O'Toole, E. T., Winey, M., Salmon, E. D., Casey, P. J., Nelson, W. J. and Barth, A. I. M. (2008). beta-Catenin is a Nek2 substrate involved in centrosome separation. *Gene Dev.* **22**, 91-105.

Bornens, M. (2002). Centrosome composition and microtubule anchoring mechanisms. *Curr. Opin. Cell Biol.* **14**, 25-34.

Bornens, M. (2012). The centrosome in cells and organisms. *Science* **335**, 422-426.

Cao, J., Shen, Y., Zhu, L., Xu, Y., Zhou, Y., Wu, Z., Li, Y., Yan, X. and Zhu, X. (2012). miR-129-3p controls cilia assembly by regulating CP110 and actin dynamics. *Nat. Cell Biol.* **14**, 697-706.

Decarreau, J., Wagenbach, M., Lynch, E., Halpern, A. R., Vaughan, J. C., Kollman, J. and Wordeman, L. (2017). The tetrameric kinesin Kif25 suppresses pre-mitotic centrosome separation to establish proper spindle orientation (vol 19, pg 384, 2017). *Nat. Cell Biol.* **19**, 740-740.

Fang, G., Zhang, D., Yin, H., Zheng, L., Bi, X. and Yuan, L. (2014). Centlein mediates an interaction between C-Nap1 and Cep68 to maintain centrosome cohesion. *J. Cell Sci.* **127**, 1631-1639.

Freire-Aradas, A., Phillips, C., Mosquera-Miguel, A., Girón-Santamaría, L., Gómez-Tato, A., Casares de Cal, M., Álvarez-Dios, J., Ansede-Bermejo, J., Torres-Español, M., Schneider, P. M. et al. (2016). Development of a methylation marker set for forensic age estimation using analysis of public methylation data and the Agena Bioscience EpiTYPER system. *Forensic Sci. Int. Genet.* **24**, 65-74.

Fry, A. M. (2002). The Nek2 protein kinase: a novel regulator of centrosome structure. *Oncogene* **21**, 6184-6194.

Fry, A. M., Meraldi, P. and Nigg, E. A. (1998). A centrosomal function for the human Nek2 protein kinase, a member of the NIMA family of cell cycle regulators. *EMBO J.* **17**, 470-481.

Graser, S., Stierhof, Y.-D. and Nigg, E. A. (2007). Cep68 and Cep215 (Cdk5rap2) are required for centrosome cohesion. *J. Cell Sci.* **120**, 4321-4331.

Hames, R. S. and Fry, A. M. (2002). Alternative splice variants of the human centrosome kinase Nek2 exhibit distinct patterns of expression in mitosis. *Biochem. J.* **361**, 77-85.

He, R., Huang, N., Bao, Y., Zhou, H., Teng, J. and Chen, J. (2013). LRRC45 is a centrosome linker component required for centrosome cohesion. *Cell Rep.* **4**, 1100-1107.

Helps, N. R., Luo, X., Barker, H. M. and Cohen, P. T. W. (2000). NIMA-related kinase 2 (Nek2), a cell-cycle-regulated protein kinase localized to centrosomes, is complexed to protein phosphatase 1. *Biochem. J.* **349**, 509-518.

Hosoda, Y., Yoshikawa, M., Miyake, M., Tabara, Y., Shimada, N., Zhao, W., Oishi, A., Nakanishi, H., Hata, M., Akagi, T. et al. (2018). CCDC102B confers risk of low vision and blindness in high myopia. *Nat. Commun.* **9**, 1782.

Kim, K., Lee, S., Chang, J. and Rhee, K. (2008). A novel function of CEP135 as a platform protein of C-NAP1 for its centriolar localization. *Exp. Cell Res.* **314**, 3692-3700.

Loukil, A., Tormanen, K. and Sütterlin, C. (2017). The daughter centriole controls ciliogenesis by regulating Neurl-4 localization at the centrosome. *J. Cell Biol.* **216**, 1287-1300.

Lüders, J. and Stearns, T. (2007). Opinion - Microtubule-organizing centres: a re-evaluation. *Nat. Rev. Mol. Cell Biol.* **8**, 161-167.

Mahen, R. (2018). Stable centrosomal roots disentangle to allow interphase centriole independence. *PLoS Biol.* **16**, e2003998.
Man, X., Megraw, T. L. and Lim, Y. P. (2015). Cep68 can be regulated by Nek2 and SCF complex. *Eur. J. Cell Biol.* **94**, 162-172.
Mardin, B. R. and Schiebel, E. (2012). Breaking the ties that bind: new advances in centrosome biology. *J. Cell Biol.* **197**, 11-18.
Mayor, T., Stierhof, Y.-D., Tanaka, K., Fry, A. M. and Nigg, E. A. (2000). The centrosomal protein C-Nap1 is required for cell cycle-regulated centrosome cohesion. *J. Cell Biol.* **151**, 837-846.
Mayor, T., Hacker, U., Stierhof, Y. D. and Nigg, E. A. (2002). The mechanism regulating the dissociation of the centrosomal protein C-Nap1 from mitotic spindle poles. *J. Cell Sci.* **115**, 3275-3284.
Mazo, G., Soplop, N., Wang, W.-J., Uryu, K. and Tsou, M.-F. B. (2016). Spatial control of primary ciliogenesis by subdistal appendages alters sensation-associated properties of cilia. *Dev. Cell* **39**, 424-437.
Meraldi, P. and Nigg, E. A. (2001). Centrosome cohesion is regulated by a balance of kinase and phosphatase activities. *J. Cell Sci.* **114**, 3749-3757.
Nam, H.-J. and van Deursen, J. M. (2014). Cyclin B2 and p53 control proper timing of centrosome separation. *Nat. Cell Biol.* **16**, 535-546.
Nechipurenko, I. V., Olivier-Mason, A., Kazatskaya, A., Kennedy, J., McLachlan, I. G., Heiman, M. G., Blacque, O. E. and Sengupta, P. (2016). A conserved role for girdin in basal body positioning and ciliogenesis. *Dev. Cell* **38**, 493-506.
Nigg, E. A. (2006). Cell biology: a licence for duplication. *Nature* **442**, 874-875.
Nigg, E. A. and Stearns, T. (2011). The centrosome cycle: centriole biogenesis, duplication and inherent asymmetries. *Nat. Cell Biol.* **13**, 1154-1160.
Pagan, J. K., Marzio, A., Jones, M. J. K., Saraf, A., Jallepalli, P. V., Florens, L., Washburn, M. P. and Pagano, M. (2015). Degradation of Cep68 and PCNT cleavage mediate Cep215 removal from the PCM to allow centriole separation, disengagement and licensing. *Nat. Cell Biol.* **17**, 31-43.
Panic, M., Hata, S., Neuner, A. and Schiebel, E. (2015). The centrosomal linker and microtubules provide dual levels of spatial coordination of centrosomes. *PLoS Genet.* **11**, e1005243.
Park, J.-L., Kim, J. H., Seo, E., Bae, D. H., Kim, S.-Y., Lee, H.-C., Woo, K.-M. and Kim, Y. S. (2016). Identification and evaluation of age-correlated DNA methylation markers for forensic use. *Forensic Sci. Int. Genet.* **23**, 64-70.
Tsou, M.-F. B. and Stearns, T. (2006). Mechanism limiting centrosome duplication to once per cell cycle. *Nature* **442**, 947-951.
Vlijm, R., Li, X., Panic, M., Rüthnick, D., Hata, S., Herrmannsdörfer, F., Kuner, T., Heilemann, M., Engelhardt, J., Hell, S. W. et al. (2018). STED nanoscopy of the centrosome linker reveals a CEP68-organized, periodic rootletin network anchored to a C-Nap1 ring at centrioles. *Proc. Natl. Acad. Sci. USA* **115**, E2246-E2253.
Yang, J., Adamian, M. and Li, T. S. (2006). Rootletin interacts with C-Nap1 and may function as a physical linker between the pair of centrioles/basal bodies in cells. *Mol. Biol. Cell* **17**, 1033-1040.
Zayed, H., Chao, R., Moshrefi, A., Lopezjimenez, N., Delaney, A., Chen, J., Shaw, G. M. and Slavotinek, A. M. (2010). A maternally inherited chromosome 18q22.1 deletion in a male with late-presenting diaphragmatic hernia and microphthalmia-evaluation of DSEL as a candidate gene for the diaphragmatic defect. *Am. J. Med. Genet. A* **152A**, 916-923.
Zhao, H., Zhu, L., Zhu, Y., Cao, J., Li, S., Huang, Q., Xu, T., Huang, X., Yan, X. and Zhu, X. (2013). The Cep63 paralogue Deup1 enables massive de novo centriole biogenesis for vertebrate multiciliogenesis. *Nat. Cell Biol.* **15**, 1434.